Supporting Information

Raman and Infrared Phonon Features in a Designed Cubic Polymorph of $CaTa_2O_6$

N.G. Teixeira, R.L. Moreira, R.P.S.M. Lobo, M.R.B. Andreeta, A.C. Hernandes

and A. Dias

Micrographs of the single crystal sample used in the X-ray, infrared and Raman experimental setups are showed, aiming to give a better view of the used orientations in the polarized experiments. A summary of the individual Lorentz lines used in peak fitting of the Raman spectra for different scattering geometries complete this supplementary material.

Figure S1, below, presents a $CaTa_2O_6$ single crystal fiber mounted for the X-ray measurements. The parallelepiped (red) edges show the crystalline directions: the vertical axis, labeled as [001] (// *z*), and the perpendicular (*a* or *b*) directions of the cubic *Pm*3 symmetry. The face in the plane of the figure is normal to the direction *d'* = [1$\bar{1}$0]. This plane, called *dz*, contains the longitudinal *z*-axis and a transversal *d*-axis (// [110]).

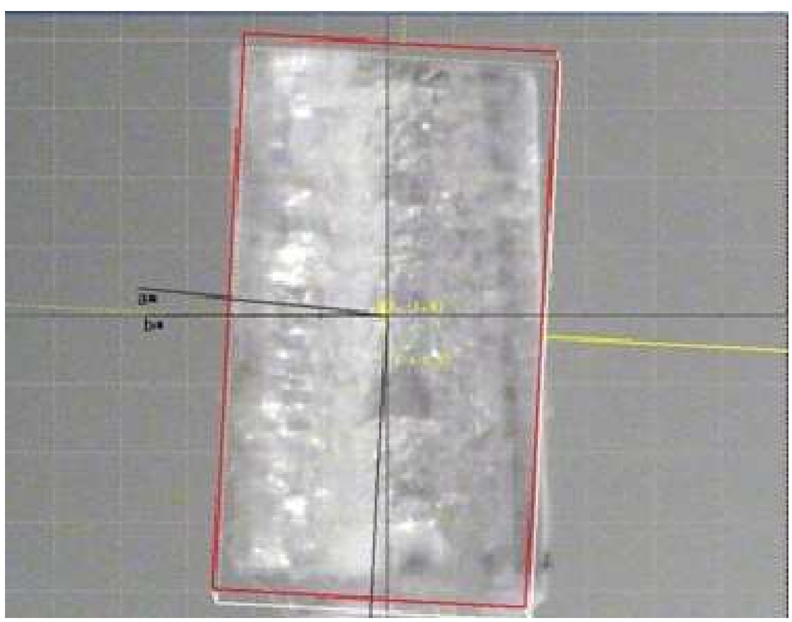

Fig. S1: Crystallographic orientation of the $CaTa_2O_6$ single crystal fiber. The crystal, already cut and polished, is 800 μm long with a 400 μm diameter.

Micro-infrared spectroscopic measurements of the single crystal fiber were done in the *dz*-plane, with or without appropriate polarizers for far and mid-infrared regions. The measuring region (300 μm × 300 μm) and the crystal orientation are shown in Fig. S2.

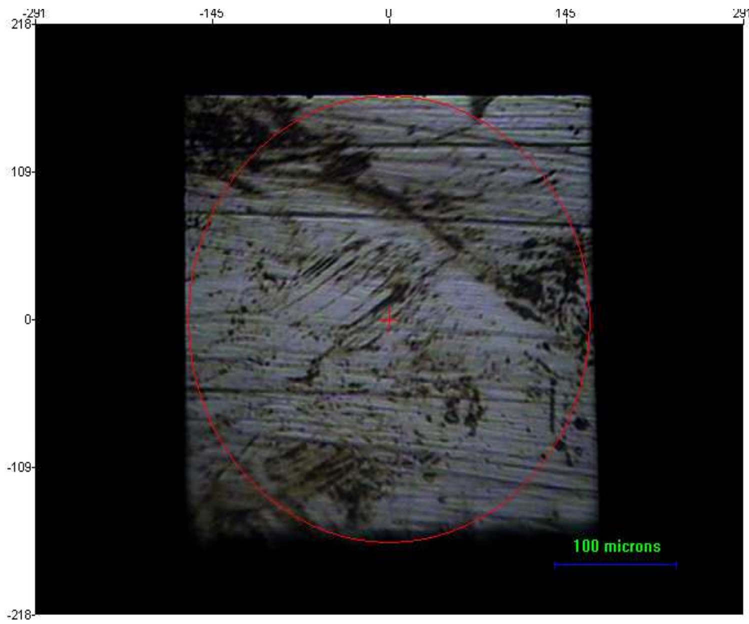

Fig. S2: *In-situ* microphotography of the $CaTa_2O_6$ fiber cut and polished in the *dz*-plane (the *z*-axis is along the horizontal direction). Polarized infrared measurements were done with the light electrical field parallel to the *z*-axis.

The Raman measurements were done on a (polished) transversal cross-section of the $CaTa_2O_6$ crystal fibers. The fibers were cylindrical, with small facets which revealed to be parallel to the cubic unit cell edges (minor facets) or to the <110> directions (major ones). Fig. S3 shows two micrographs with the (*in-situ*) crystal orientations for the polarized Raman experiments. In the left photography, note a natural *dz*-facet on the left (vertical direction) and the polished *dz*-surface (used for infrared measurements) on the right.

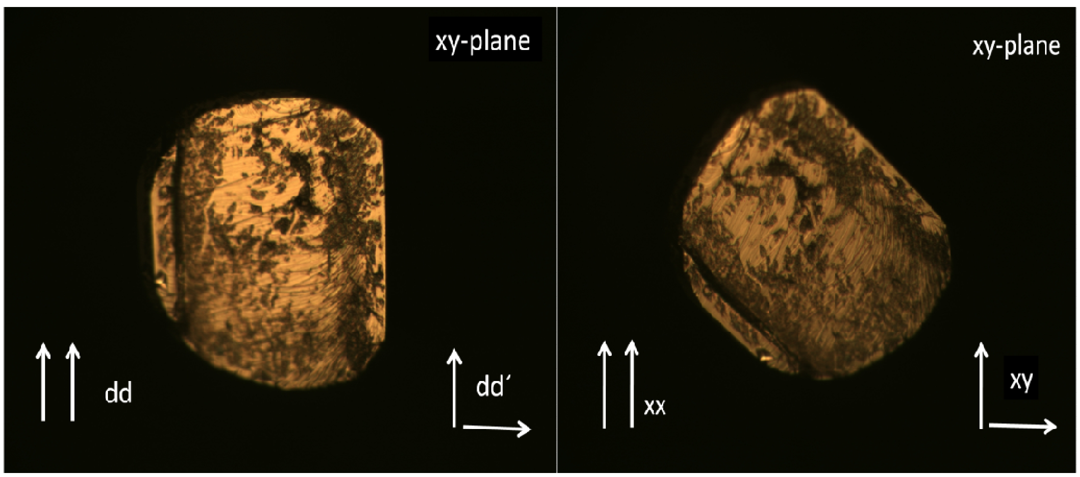

Fig. S3: In-situ micrographs of the oriented $CaTa_2O_6$ sample for the Raman experiments. The four scattering geometries used are indicated by the arrows.

Table S1 shows the obtained fitting parameters for the Raman spectra, in the four scattering configurations chosen (peak positions and half-width at half-maxima, HWHM, of the Lorentz lines are given in cm^{-1}). This table must be taken carefully, for it does not show the intensities. The leakage peaks are important to the fittings, but are weaker than the allowed ones. The code of colors for the irreducible representations is the same used in the figures of the paper.

Table S1- The depicted Raman modes of the $CaTa_2O_6$ single crystal fibers, in the four measured scattering configurations. The phonon wavenumbers and widths (HWHM) are in cm^{-1}. The individual peaks are in black (A_g), blue (E_g), red (F_{2g}) and wine (IR modes).

#	$z(xx)\bar{z}$ A_g+E_g	$z(xy)\bar{z}$ F_g	$z(dd)\bar{z}$ $A_g+E_g+F_g$	$z(dd')\bar{z}$ E_g	Attribution	Ferrari*
1	127.5 (10.2)	-	126.8 (9.0)	131.5 (12.9)	A_g	118
2	-	146.7 (5.5)	-	-	F_g	-
3	167.1 (17.0)	-	167.8 (16.5)	167.8 (16.5)	E_g	167
4	-	175.1 (17.7)	-	-	F_g	-
-	191.5 (16.1)	-	194.6 (15.0)	190.3 (10.5)	IR(F_u)	
5	-	214.6 (23.0)	-	212.8 (48.5)	F_g	
6	-	217.8 (22.8)	-	-	F_g	-
7	231.7 (24.0)	-	227.2 (19.0)	-	A_g	227
8	271.1 (18.8)	272.9 (18.5)	272.3 (19.7)	272.3 (19.7)	E_g	270
9	-	309.9 (25.2)	305.5 (16.3)	-	F_g	
10	317.0 (23.5)	-	316.8 (22.9)	316.8 (22.9)	E_g	317
11	363.4 (18.2)	360.0 (9.4)	360.0 (9.6)	363.0 (14.7)	F_g	372
12	427.1 (10.3)	-	-	425.5 (10.7)	F_g	-
13	461.3 (11.0)	463.7 (3.0)	459.3 (10.4)	459.3 (10.4)	E_g	463
14	490.5 (21.8)	-	485.9 (17.2)	486.8 (14.2)	F_g	-
15	-	565.2 (10.9)	565.3 (10.9)	-	F_g	-
16	-	579.1 (12.7)	-	-	F_g	
17	596.9 (18.2)	598.8 (18.3)	590.5 (21.8)	601.8 (29.1)	E_g	591
18	645.4 (40.6)	638.7 (20.6)	641.8 (28.7)	641.8 (28.7)	A_g	650
19	-	667.3 (11.5)	667.3 (11.5)	667.8 (18.8)	F_g	-
20	740.4 (36.7)	-	741.6 (29.9)	736.5 (28.2)	A_g	-
21	843.8 (42.4)	-	850.2 (43.5)	856.4 (88.1)	A_g	856
-	890.0 (33.7)	-	900.9 (31.7)	-	IR(F_u)	
-	942.9 (26.4)	-	948.8 (20.4)	-	IR(F_u)	

*C. R. Ferrari *et al.* (ref. 3), *J. Cryst. Growth* **2004**, *266*, 475.